

LASER INTERFEROMETER GRAVITATIONAL WAVE OBSERVATORY  
- LIGO -  
CALIFORNIA INSTITUTE OF TECHNOLOGY  
MASSACHUSETTS INSTITUTE OF TECHNOLOGY

<b>Technical Note</b>	<b>LIGO-T1800200-vX</b>	2018/09/19
<b>In Situ Laser Mode Spectroscopy for Mirror Phase Mapping</b> <b>Interim Report 2</b>		
Sandrine Ferrans Mentors: Gautam Venugopal, Koji Arai and Rana Adhikari		

**California Institute of Technology**  
**LIGO Project, MS 18-34**  
**Pasadena, CA 91125**  
Phone (626) 395-2129  
Fax (626) 304-9834  
E-mail: info@ligo.caltech.edu

**Massachusetts Institute of Technology**  
**LIGO Project, Room NW22-295**  
**Cambridge, MA 02139**  
Phone (617) 253-4824  
Fax (617) 253-7014  
E-mail: info@ligo.mit.edu

**LIGO Hanford Observatory**  
**Route 10, Mile Marker 2**  
**Richland, WA 99352**  
Phone (509) 372-8106  
Fax (509) 372-8137  
E-mail: info@ligo.caltech.edu

**LIGO Livingston Observatory**  
**19100 LIGO Lane**  
**Livingston, LA 70754**  
Phone (225) 686-3100  
Fax (225) 686-7189  
E-mail: info@ligo.caltech.edu

# 1 Abstract

The LIGO detectors are Michelson based interferometers with Fabry Perot cavities. The Fabry Perot cavities in aLIGO creates an optical resonator with semi-transparent spherical mirrors, where light is reflected and transmitted before being merged into an interference pattern for output. However, the mirrors are not perfect and contain surface defects which contribute to optical losses. This project is focused on improving the optics in LIGO by characterizing mirror figure error that contribute to optical losses. As a result of scattered light, optical losses increase shot noise and destroy the squeeze state of light. Surface perturbations will be evaluated with In-Situ mode spectroscopy, so the gravitational wave output will not be affected. Mirror figure error will cause the resonant frequencies of the Hermite Gaussian modes to shift from their ideal theoretical spacings. Mirror phase maps, a physical representation of the mirror, can be reconstructed by analyzing the shift in transverse mode spacings with Bayesian inference techniques. The success of aLIGO is largely due to precise optical measurements. By mapping the physical surface of the mirror down to 1 Angstrom, the surface perturbations contributing to optical losses will be mapped.

## 2 Introduction

### 2.1 Gravitational Waves

Einstein predicted gravitational waves in his theory of General Relativity, which states that gravity is the distortion of spacetime due to the presence of mass. Mass creates a curvature in the geometry of spacetime. Gravitational waves are ripples in the fabric of spacetime, and these waves distort spacetime geometry as they propagate at the speed of light. Gravitational waves interact with matter by stretching in one direction and compressing space in the perpendicular direction. They originate from the acceleration of large masses, specifically from cataclysmic cosmic events such as the collision of black holes. Gravitational waves are important because they carry information about their origin, the universe, and the nature of gravity itself.

### 2.2 LIGO

LIGO (Laser Interferometer Gravitational Wave Observatory) is a gravitational wave detector in Livingston, Louisiana, and in Hanford, Washington. LIGO is a Michelson based interferometer with Fabry Perot cavities. The interferometer creates an interference pattern from the constructive or deconstructive interference of waves. The interferometer has two perpendicular arms of equal length. The laser beam will take the same time to travel the same distance, which will produce deconstructive interference, where the light waves cancel each other out. Thus, the photodetector will not detect a light pattern. However, when a gravitational wave passes, the length of the arms changes. One arm is stretched, and the other one is compressed. The photodetector will detect an interference pattern due to the changes in relative length between the masses. Gravitational waves will alter the time the light will travel in the interferometer. The difference in time will produce an interference pattern in which astronomical information can be extracted.

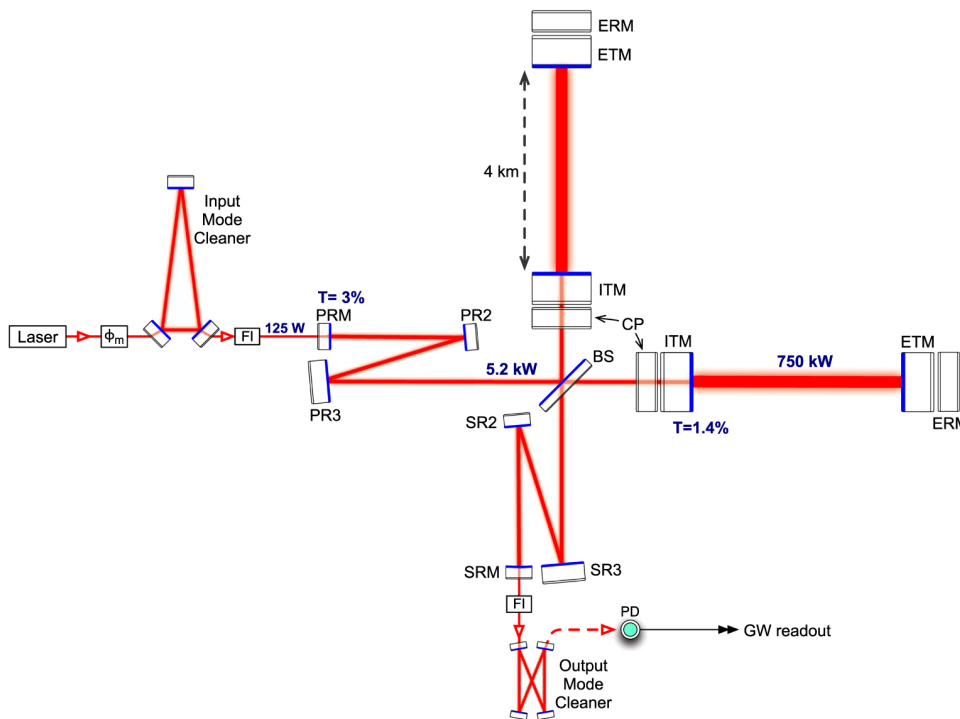


Figure 1: Schematic diagram of Advanced LIGO

The arms of LIGO are 4 km long. Incorporating Fabry Perot cavities into each arm increases the sensitivity by increasing the interaction time of the gravitational wave with the interferometer. This can be done by introducing additional mirrors near the beam splitter, causing the each part of the laser beam to reflect 280 times before being merged into an interference pattern [?].

### 2.3 Optical Losses

The success of Advanced LIGO is largely due to precise optical measurements which result in the sensitivity to detect gravitational waves. This project is focused on improving the optics in LIGO by characterizing mirror figure error that contribute to optical losses. Optical losses are a result of light scattering. Defects, absorption, microroughness, transmission by the end test mass, and mirror figure error cause light scattering. Mirror figure error has a low spatial frequency, which causes a low scattering angle of light [?]. Scattered light alters the amplitude and phase of the laser used for gravitational wave detection.

The project is aimed to reduce optical power losses due to mirror figure error. The requirements of Advanced LIGO are that the round trip cavity loss must be less than 75 parts per million [?].

Mirror figure error is the second largest contributor to optical losses, with a budget of 24 ppm for the combination of both test masses [?]. Optical losses destroy the squeezed state of light, reduce the circulating power in the cavities, which increases shot noise in the data. Shot noise is considered quantum noise in LIGO's noise budget. Quantum noise is one of the

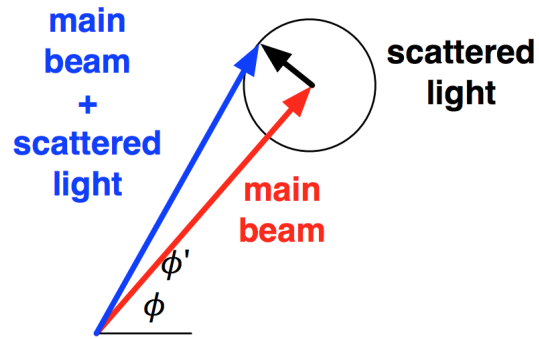


Figure 2: The Scattered Light on LIGO's beam used for interferometry

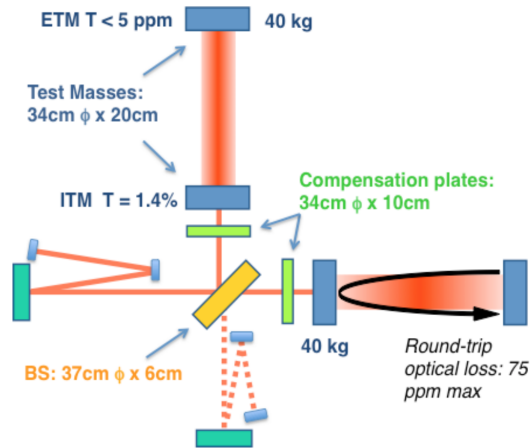


Figure 3: The Optical Loss Round Trip in LIGO's interferometric beam

highest noise contributors. Thus, it is highly important for LIGO to reduce optical losses in order to achieve the sensitivity to detect gravitational waves.

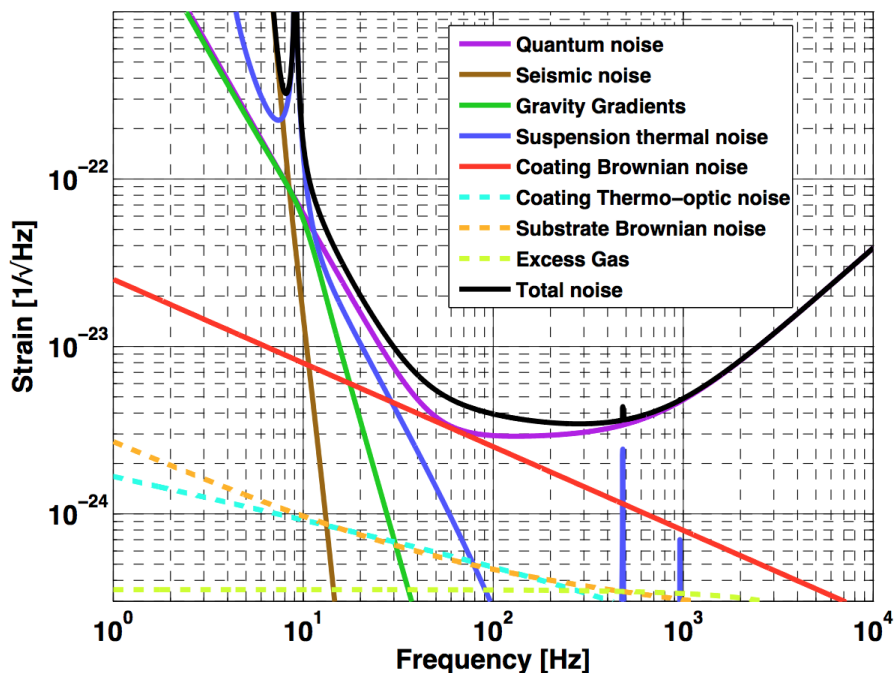


Figure 4: The Noise Budget of Advanced LIGO

We will develop an in-situ technique to characterize mirror figure error using an optical cavity, which will be demonstrated on the Y arm of the 40m prototype at Caltech. Ultimately, we will measure the transverse mode spacings and create mirror phase maps.

## 2.4 Optical Resonators

### 2.4.1 Fabry Perot Cavity

An optical resonator is a system that consists of two mirrors (ITM and ETM) that form a standing wave. A cavity eigenmode describes the standing wave pattern, which is the light pattern that is continuously reflected. Only certain modes are allowed to resonate inside of the cavity.

The Fabry Perot Cavity used in Advanced LIGO is an optical resonator with spherical mirrors. There are two types of modes: longitudinal modes and transverse modes. Longitudinal modes describe the laser frequency and determine the certain frequencies that are allowed to resonant inside of the cavity. Longitudinal modes are determined by the absolute length of the cavity. A transverse mode differs in frequency and amplitude, and it depends on the radius of the curvature of the mirrors.

A system with perfectly spherical mirrors has Gaussian modes. A Gaussian mode is a transverse mode, and the intensity of light can be described in a Gaussian distribution function.

Parameter	Value
Cavity length (L)	40 m
ITM Reflectivity (R)	0.98616
ITM Transmissivity (T)	0.01384
ETM Reflectivity (R)	0.9999863
ETM Transmissivity (T)	$1.37 \times 10^{-6}$
ITM Radius of curvature ( $R_1$ )	$\infty$
ETM Radius of curvature ( $R_2$ )	60 m

Table 1: Parameters of the 40m prototype LIGO interferometer.

The fundamental Gaussian mode has repetitive resonances with the laser frequency of the Free Spectral Range (FSR), which describes the spaces between two resonant longitudinal modes. The FSR is defined as,

$$\nu_{FSR} = \frac{c}{2L} = 3.7474 \times 10^6 \text{ Hz}$$

The FSR is determined by the absolute length of the cavity. The FSR is known as the fundamental mode of resonance or TEM00.

### 2.4.2 Hermite Gaussian Modes

A Hermite Gaussian mode is a higher order mode that has an intensity distribution that differs from the fundamental Gaussian mode. Hermite Gaussian modes are described by spacial indices (n,m) for TEM<sub>nm</sub>. Hermite Gaussian modes describe electrical field distributions, composed of a Hermite Polynomial and a Gaussian function.

$$E_{nm}(x, y, z) = E_0 \frac{w_0}{w(z)} H_n \left( \frac{\sqrt{2}x}{w(z)} \right) H_m \left( \frac{\sqrt{2}y}{w(z)} \right) \exp \left( -\frac{x^2 + y^2}{w(z)^2} \right) \exp \left( -i \left[ kz - (1 + n + m) \arctan \left( \frac{z}{z_R} \right) + \frac{k(x^2 + y^2)}{2R(z)} \right] \right)$$

Where:

- $E_0$  is the electric field amplitude,
- $H_n$  is the  $n$ th order polynomial,
- $W_0$  represents the beam waist,
- $W(z)$  is the beam radius along the  $z$ -axis,
- $R(z)$  represents the radius of curvature of the wavefront,
- $z_R$  is the Rayleigh range, or the distance along the  $z$ -axis at which the wavefronts of the beam are most curved, and is defined as  $z_R = \frac{\pi W_0^2}{\lambda}$ ,

The Hermite Gaussian modes as a representation of the electric field distributions of a beam are analogous to the energy perturbations in a simple quantum harmonic oscillator. The energy in a harmonic oscillator is composed of a one dimensional Hermite polynomial, and the electric field amplitudes of a beam is a two dimensional problem with two Hermite polynomials.

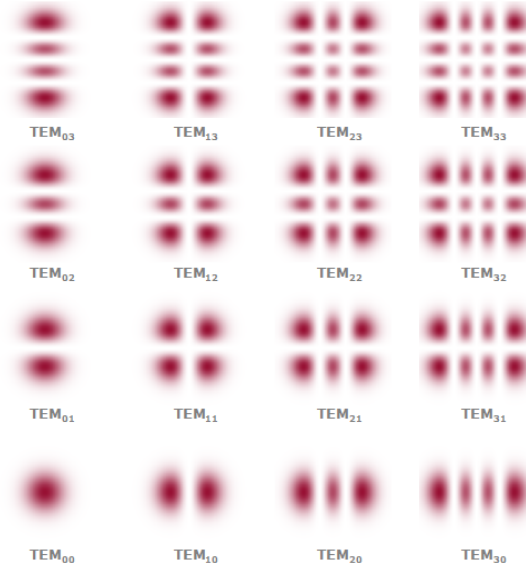


Figure 5: Hermite Gaussian Modes

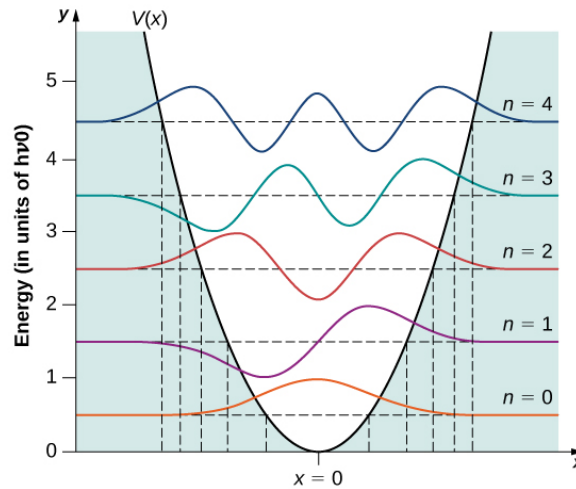


Figure 6: Hermite Gaussian Modes

The Transverse Mode Spacing (TMS) is the distance between transverse modes. The higher order modes have a frequency separation of multiples of the transverse mode spacing from the fundamental mode of resonance.

$$\nu_{TMS} = \nu_{FSR} \times \left(\frac{n+m}{\pi}\right) \cos^{-1} \sqrt{g_1 g_2}$$

Mirror figure error causes a shift in the frequency spacings. Thus, information about mirror figure error will be extracted by precisely measuring the shift of the transverse mode frequencies.

The  $g$  parameters depend on the absolute length of the cavity and the radius of curvature of the mirrors.

$$g_1 = 1 - \frac{L}{R_1} \approx 1$$

$$g_2 = 1 - \frac{L}{R_2} \approx 0.298$$

The Gouy Phase is  $\Delta\varphi$ ,

$$\Delta\varphi = \varphi(z_2) - \varphi(z_1) = \cos^{-1} \pm \sqrt{g_1 g_2}. \quad (1)$$

The Gouy Phase is stronger for HOMs, which can cause the resonant frequencies to be higher.

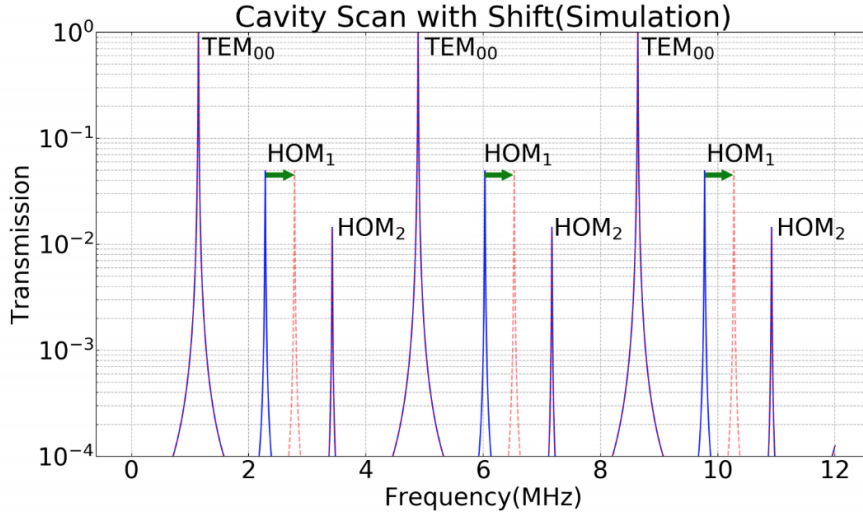


Figure 7: Exaggerated Shift in Resonant Frequencies of Higher Order Modes due to Figure Error

### 3 Objectives

The goal of this project is to create a mirror map that characterizes the figure error on the test masses causing optical losses. A mirror map visually depicts the imperfections on the surface of the mirror. Mirror maps are conventionally created using Fizeau interferometry. However, Fizeau interferometry would effect the gravitational wave detector's output. Thus, we will use an in-situ technique through mode spectroscopy because this research will be applied to measure the mirror figure error in LIGO's gravitational wave detectors.



A cavity scan will be performed by injecting an auxiliary laser into the 40m LIGO prototype interferometer to measure its transverse mode spacings. The transverse mode spacings obtained experimentally will be compared to an ideal model simulated in Finesse in order to analyze the shift in resonant frequencies. A heater will be installed in the ETM of the Y arm to create a known perturbation in the mirror. This will be done in order to check our Bayesian inference and the Monte Carlo Chain Method will be used to characterize the most probable perturbations of the cavity mirrors and create a high resolution mirror map for the input test mass (ITM) and end test mass (ETM). A mirror map will be a successful outcome of the project because we will be able to identify the mirror figure error causing the optical power losses.

## 4 Approach

### 4.1 Mode Spectroscopy

Mode spectroscopy is a technique to measure the frequency of a laser and its higher order modes. This will be performed with an in-situ technique using an auxiliary laser (AUX) in 40m prototype interferometer in order to measure mode spacings. Therefore the interferometer will consist of the two beams: the pre stabilized laser (PSL), which is the beam that is used for the detection of gravitational waves, and the auxiliary laser. It is important to note that the auxiliary laser will not disturb the output of the interferometer, and therefore the mode spectroscopy can be performed while the interferometer is observing. Mode spectroscopy will be performed to measure the FSR and TMS. The FSR and TMS are determined by the frequency and the absolute length of the cavity. Thus, we rely on very accurate and precise measurements of the frequency and length of the cavity in order to determine the modes. However, the laser frequency and the arm cavity length are not stable enough to sustain the resonance of the cavity. Thus, feedback control will be used on either the frequency and the arm length using a Phase Lock Loop (PLL) and the Pound Drever Hall technique (PDH). Feedback control ensures that the PSL remains locked in the cavity.

The goal of the PLL is to reduce frequency and arm length fluctuations in order to obtain precise and accurate frequency scans, as well as to ensure that the PSL will resonate within the cavity and that the phase difference between the PSL and AUX is set. The PSL is locked using the Pound Drever Hall Locking, which stabilizes the laser by measuring the frequency with a Fabry Perot and feeding it back into the laser, ultimately suppressing frequency fluctuations [?]. The auxiliary laser will be injected from the optical port, and the will be locked to one of the arms. A beam splitter sends a small amount of the PSL and AUX beam to the PLL. The Phase Lock Loop ensures that the frequency difference between the PSL and AUX is controlled and set with a local oscillator set by the marcorni. The frequency difference between the PSL and the AUX in the PLL is set by RF generator when the PLL is locked.

The coupler sends part of the beat to the control room in order to monitor the beat frequency. The Phase Lock Loop will not lock if the beat frequency is not within a close range of the frequency set by the LO. The frequency of the beat can be altered if needed by changing the temperature of the laser. This will ensure that the PLL is in lock.

### AUX-PSL Phase-Locked Loop

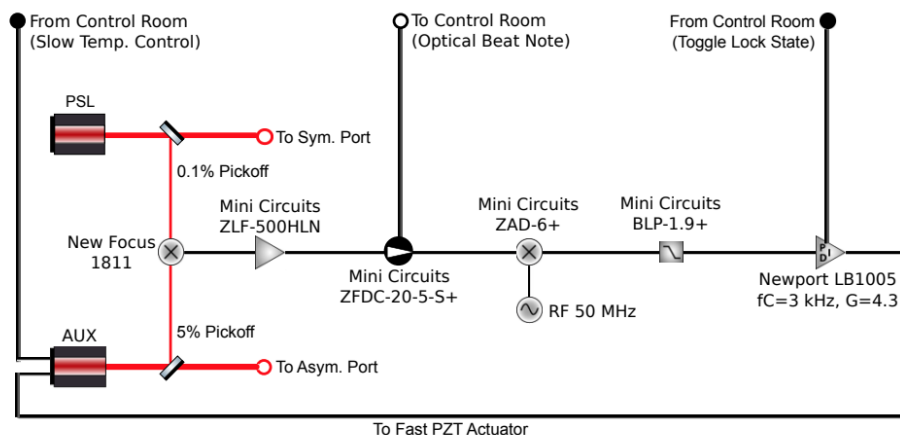


Figure 8: Schematic diagram of the AUX-PSL Phase locked loop

Currently, we have developed multiple in-situ techniques to scan the frequency of the AUX laser:

- RF offset
- AOM sidebands
- Agilent Drive Signal

The RF offset produces cavity scans by sweeping the frequency of the AUX carrier and its sidebands. The RF offset changes carrier frequency (PSL). The RF frequency goes into the AOM. The AOM created two sidebands. The sidebands resonated with the FSR and the carrier, which resulted in too much power. The sideband frequency spacings were approximately 11 mHz. It can be inferred that the repeated lines were higher order modes (HOM) due to the equal spacing. However, the frequency scan using the RF offset was unsuccessful because it was an incoherent measurement. The sidebands resonated with the FSR and the carrier, which resulted in too much power.

The goal of scanning the frequency using the AOM sidebands was to create a coherent and sentinel measurement. A transfer function will be created in order to measure the input power of the beam relative to the output of the beam at a specific frequency. This creates a pure measurement of the spectral power density. Therefore we are only looking at specific frequencies. The PSL is set to resonate within the cavity. The AOM creates two sidebands and sweeps outworks. However, the AOM sidebands technique was inconclusive because HOM's were unclear. Thus, we inserted a razor blade to add more power to the HOMs, but it was also unsuccessful. The photodetector (PD) measures the light going into the interferometer and the light after the AOM.

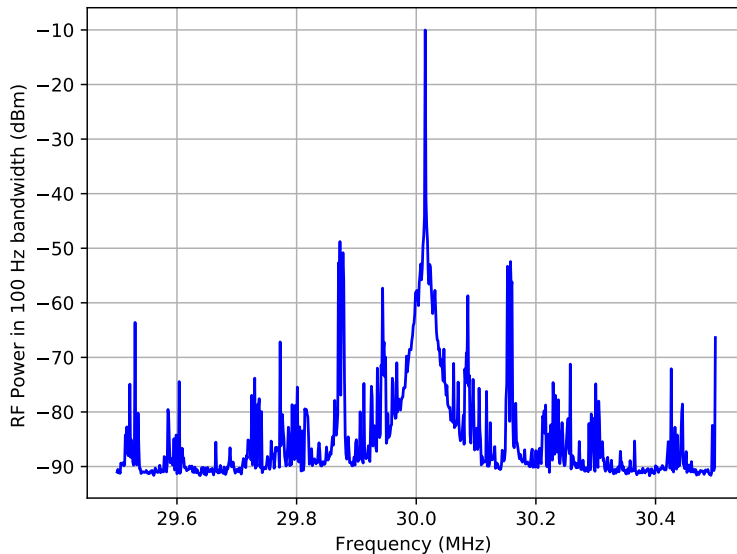


Figure 9: Power Spectral Density using the AOM sidebands

The Agilent Drive Signal swept the AUX carrier frequency. The previous methods relied on the frequency of the AM sidebands being swept, and the carrier was locked at a fixed offset from the PSL carrier. 1/3 of the output aux beam was clipped by inserting a razor blade. This was done so the PDA255 will witness more higher order modes by disrupting the symmetry of the output.

We used this method with a double demodulation and simplified it further to a single demodulation.

## 4.2 Heater

### 4.3 Set Up

Two heaters will be installed to radiate electromagnetic radiation in the ETM of the Y arm in order to create a perturbation in the mirror. We will be purposefully inserting known perturbations into the mirror in order to observe a shift in higher order modes.

The transverse mode spacings depend on the radius of curvature of the mirrors. The heater will increase the radius of curvature of the mirror, and therefore decrease the transverse mode spacings.

It is important to note that each higher order mode will have a different beam size and will therefore witness a different radius of curvature.

The heater will be inserted into an elliptical reflector. However, the reflector will be half an ellipse to ensure that it does not block the laser beam path. The reflector is an ellipse because an ellipse has two focal points. The heater will be set at one focal point, so that the heat will be radiated towards the other focal point. The focal points will be a specific point on the ETM of the Y arm and this point will create a perturbation on the mirror. This is

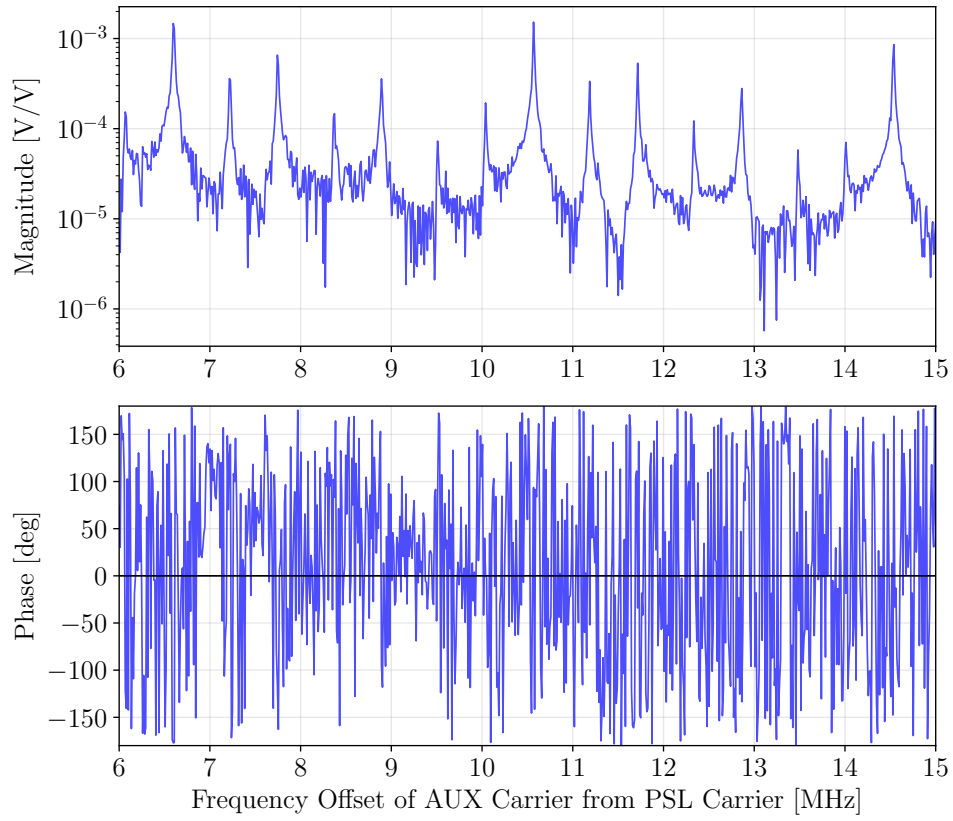


Figure 10: The Power Spectral Density using the Agilent Drive

**Phase Locked Loop – Single demodulation**

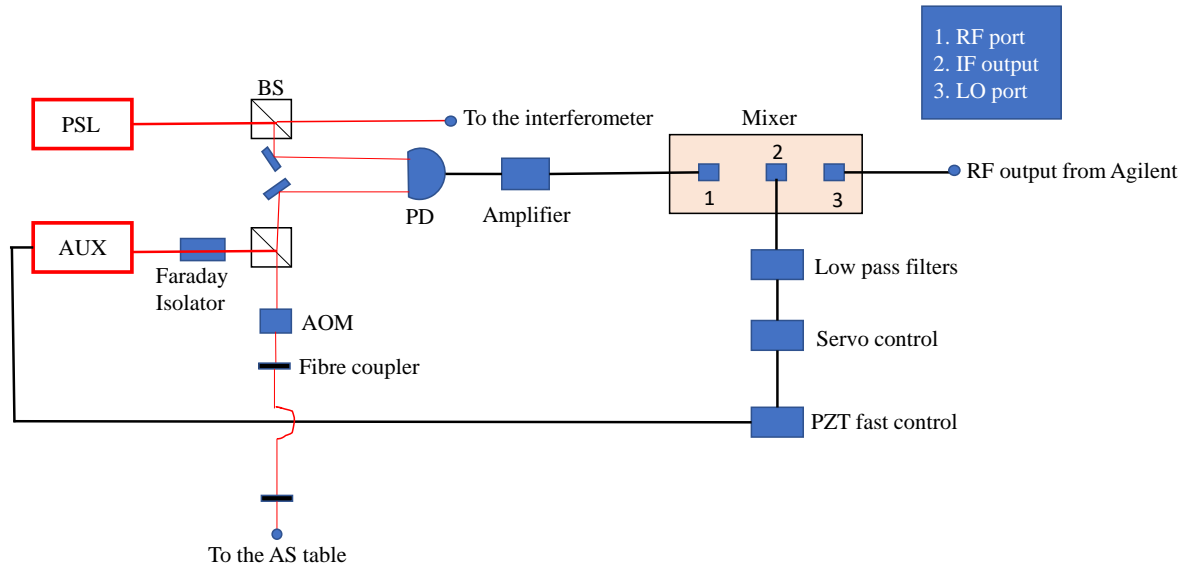


Figure 11: The Agilent Drive technique with single demodulation

**Double Demodulation technique**

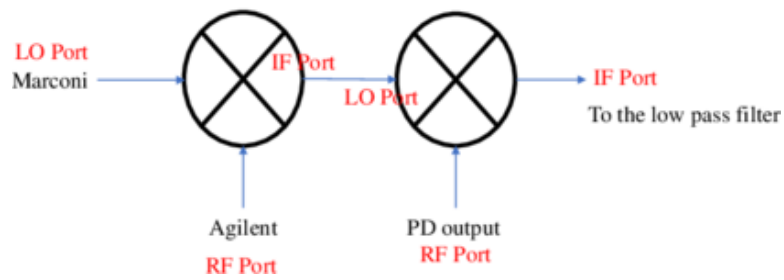


Figure 12: The Agilent Drive technique with double demodulation

to focus all of the infrared radiation and power into one point as precisely as possible.

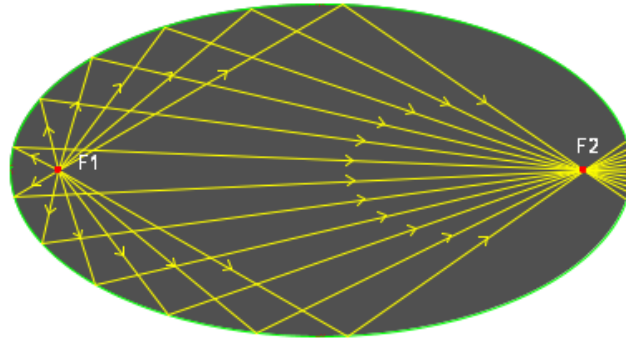


Figure 13: Ellipse, where the heater will be installed in focal point 1 and the perturbation in the ETM mirror is focal point 2.

The other heater installed in the ETMY chamber is a cylindrical heater, where the heat is focused onto two lenses. However, the heating power is very low.

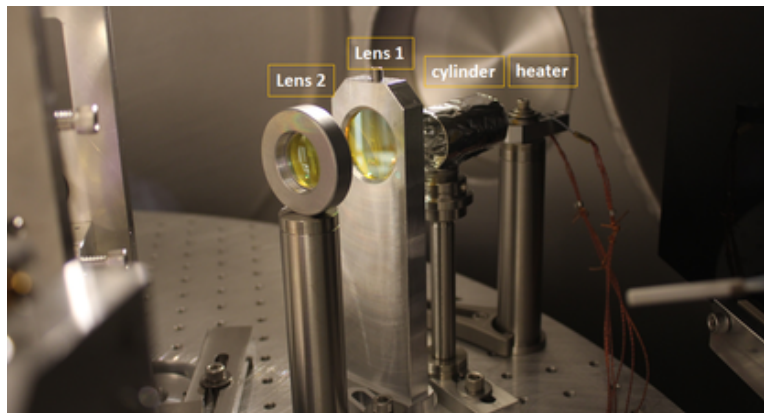


Figure 14: The cylinder + lenses projected heating pattern.

The heating pattern produced by the cylinder set up is ideal for higher order modes because each mode will witness a different radius of curvature.

The ETMY chamber will have two heaters installed: an elliptical reflector and a cylinder with two lenses. These heaters will not be on at the same time. It is important to note that the deformations in the mirror are temporary. The following figures show the set up in its entirety.

#### 4.3.1 Measurements

The tables describe the measurements taken with the heater set up.



Figure 15: The lens heating pattern.

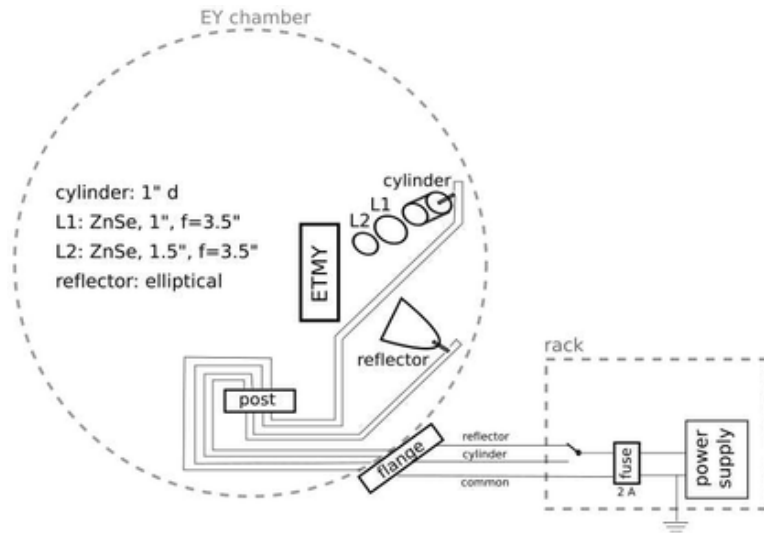


Figure 16: Schematic of heater set up in ETMY chamber.

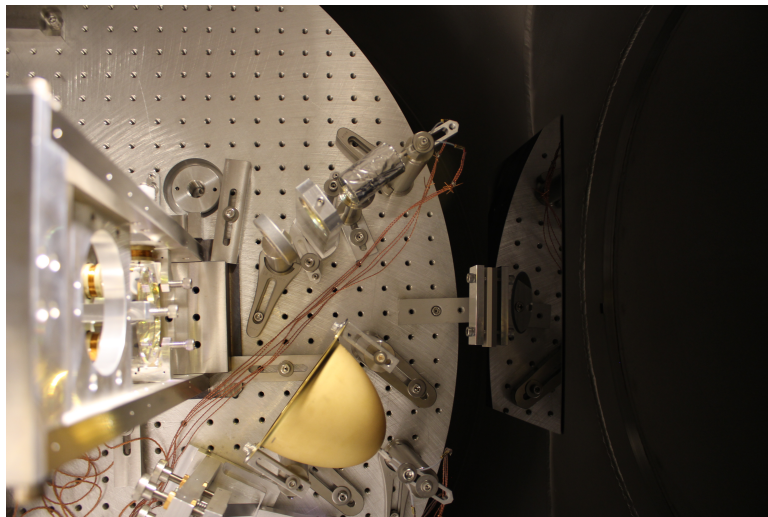


Figure 17: A picture of the current heater set up in the vacuum chamber of ETMY.

## Elliptical Reflector

Current [A]	Voltage [V]	Power [W]
0.4	2	0.8
0.5	3.4	1.7
0.6	5	3.0
0.8	9.4	7.5
0.9	12	10.8
1.09	17	18.5

## Cylinder + Lenses

Current [A]	Voltage [V]	Power [W]
0.9	15	13.5

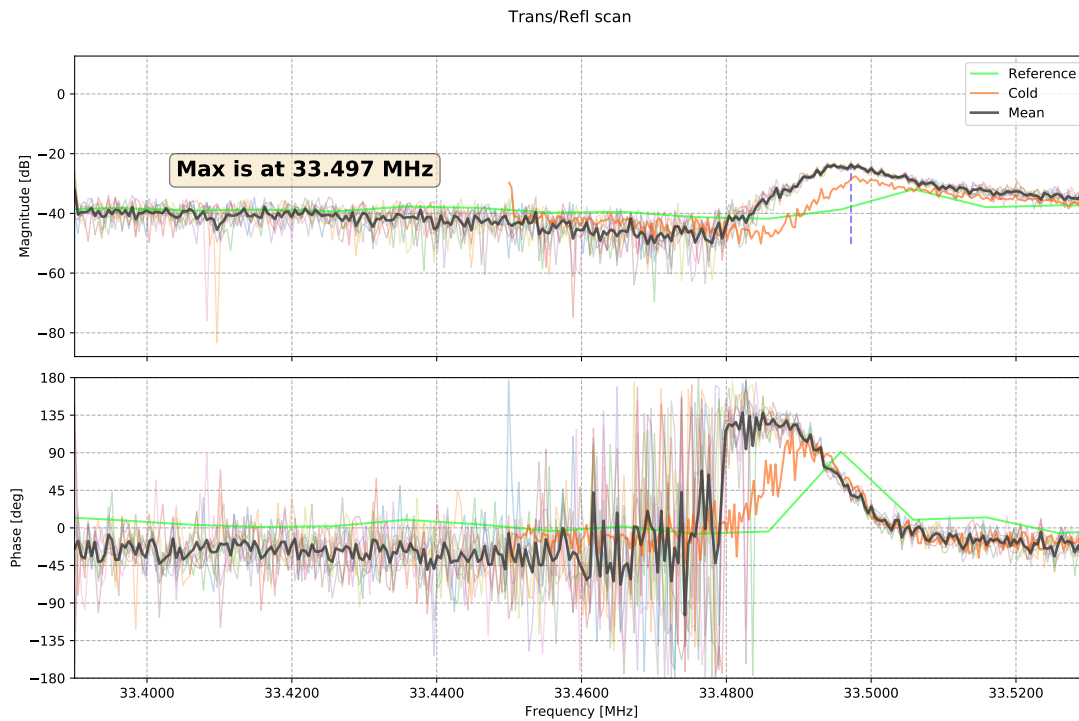


Figure 18: HOM 5 with cylindrical heater.

### 4.3.2 Magnitude Fit

The magnitude data was fitted with the equation,

$$\frac{A + B}{\sqrt{1 + \frac{X-C^2}{D}}} \quad (2)$$

- $A$  is the constant background,



- $B$  is the magnitude of the resonant peak,
- $C$  is the central position of the peak,
- $D$  is full width at half maximum.

$C$  is the most important parameter because it contains information about how much the higher order modes shifted due to perturbations on the mirror.

The fitting shows 10 Hz of magnitude resolution.

### 4.3.3 Complex Fit

The cavity scan information was obtained by measuring the magnitude and phase. Therefore, the magnitude and phase can be fitted simultaneously by reconstructing the data as a complex number. The magnitude is the real part  $Re$ , and the magnitude represents the imaginary part  $Im$ .

$$\frac{kjw^2}{\frac{w_0^2+jw_0}{Q-w^2}} \quad (3)$$

The complex reconstruction has the following properties:

- where  $k$  is the wavenumber,
- $w_0$  is the resonance frequency,
- $w$  represents the frequency,
- $Q$  is the resonance frequency divided by the full width at half maximum, which is related to the finesse of the cavity.  $Q = \frac{w_0}{FWHM}$

## 4.4 Finesse Simulations

Finesse is an optical simulation software. An ideal Fabry Perot cavity will be simulated in Finesse. The ideal model will have no figure error and the same parameters as the 40m prototype interferometer. Its transverse mode spacings will be studied and will be compared to the modes obtained experimentally to analyze the shift in the higher order modes.

Thousands of potential perturbations will be simulated in Finesse, and its effect on the optical power will be observed. Perturbations will be introduced using Zernike Polynomials coefficients. However, information about the mirror figure error cannot fully be extracted from the use of Zernike polynomials, and a mirror phase map cannot be reconstructed from the use of Zernike polynomials. Mirror phase maps can be reconstructed from the potential perturbations by using Bayesian inference.

pt8A CAR

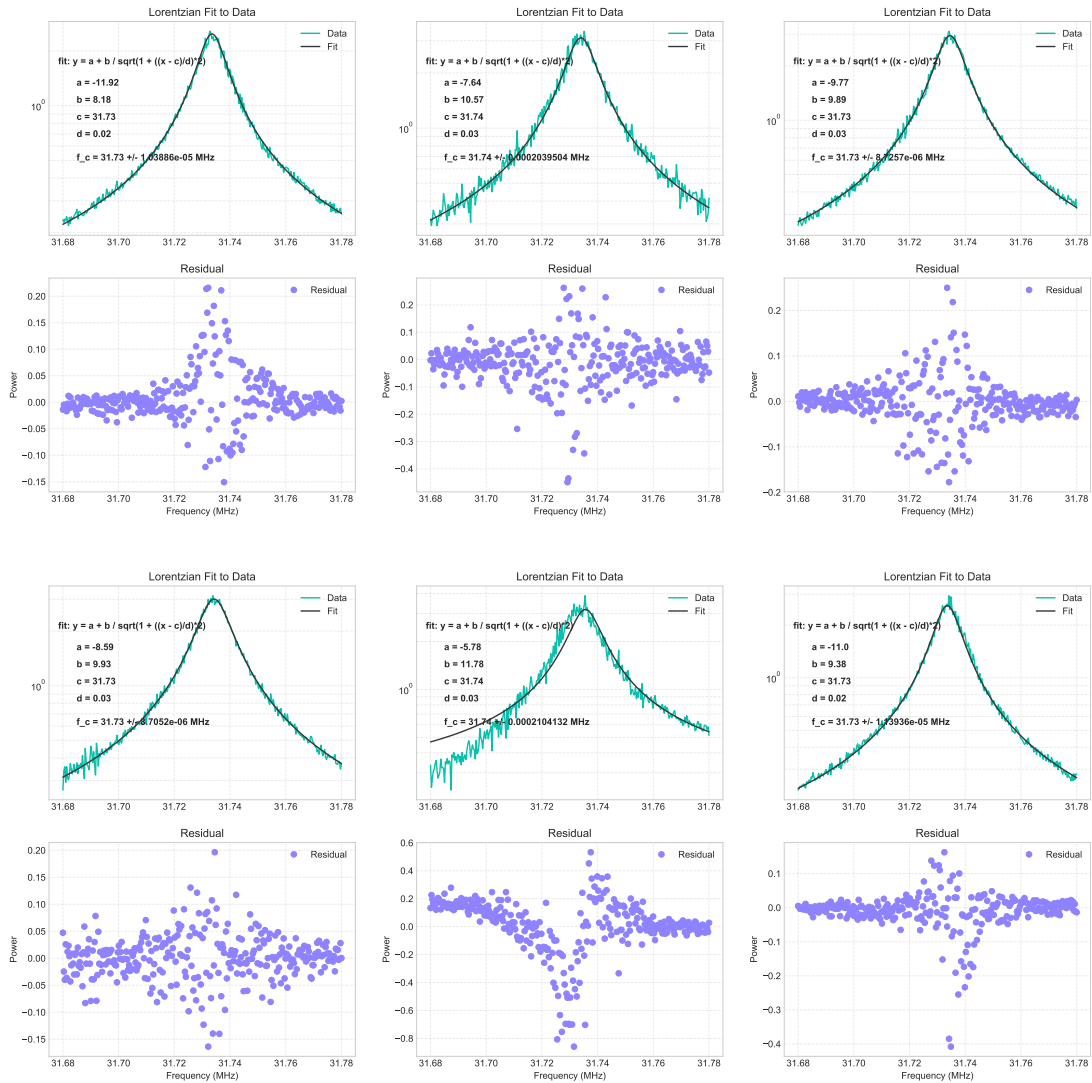


Figure 19: Fit for the carrier frequency with the cylindrical heater at 0.8A

## 4.5 Bayesian Inference

Bayesian inference will be used to produce the most probable mirror phase maps. The probability of perturbations will be continually updated as more evidence is available. What will be most important when using Bayesian inference will be understanding what causes the shift in resonant frequencies, which can tell us information about the surface defects on the mirrors. We will use Bayes' theorem of inverse problems, which will be done by analyzing the cavity transmission, then finding the most probable phase map of the cavity mirror for the given cavity scan. This relies on the Markov Chain Monte Carlo method (MCMC), which states that the future values do not depend on its previous values [?].

## 4.6 Finesse Simulations

- Create an ideal model of a Fabry Perot with no figure error using the same parameters in the 40m prototype.
  - Plot the power spectral density.
  - Use the ideal model to analyze shift in frequencies.
- Introduce mode-mismatched and misalignment into Finesse to produce a fitting model.
- Introduce figure error using Zernike polynomials and thousands of possible perturbations in mirror.
  - Observe how transmitted power is effected.

## 4.7 Creating mirror phase maps

- Evaluate optical losses as perturbations in mirrors
  - Use Monte Carlo Method to fit experimental data as a linear combination of the simulated perturbations.
- Use Bayesian Inference to investigate the most probable perturbations in the cavity mirror contributing to power losses in the interferometer. This will produce a mirror phase map.

## References

- [1] <https://www.ligo.caltech.edu/page/ligos-ifo>
- [2] Kaustubh Singhi, Koji Arai and Rana Adhikari "Mirror Metrology using Mode Spectroscopy", *LIGO-T1700195-v1*
- [3] G. Billingsley, H. Yamamoto, and L. Zhang, *Characterization of Advanced LIGO Core Optics*. <https://dcc.ligo.org/LIGO-P1700029>

- [4] Naomi Wharton, Koji Arai and Rana Adhikari, "*Laser Mode Spectroscopy for Mirror Metrology*", *LIGO-T1700195-v3*
- [5] Alberto Stochino, Koji Arai and Rana X. Adhikari, "*A Technique for In-situ Measurement of Free Spectral Range and Transverse Mode Spacing of Optical Cavities*". *LIGO DCC No. - P1200048*
- [6] Kiwamu Izumi, Koji Arai, Bryan Barr, Joseph Betzwieser, Aidan Brooks, Katrin Dahl, Suresh Doravari, Jennifer C. Driggers, W. Zach Korth, Haixing Miao, Jameson Rollins, Stephen Vass, David Yeaton-Massey and Rana X. Adhikari, "*Laser Mode Spectroscopy for Mirror Metrology*", *LIGO-T1700195-v3*
- [7] K. Arai, A. Stochino, R. Adhikari, and the LIGO 40m Lab, *Precise Measurements on Longitudinal and Transverse Mode Spacings of an Optical Cavity using an Auxiliary Laser*. <https://dcc.ligo.org/LIGO-G080647>
- [8] Eric D. Black "*An Introduction to Pound-Drever-Hall Laser Frequency Stabilization*" <https://aapt.scitation.org/toc/ajp/69/1>